Turbulence Measurements in a Compressible Reattaching Shear Layer

K. Hayakawa,* A.J. Smits,† and S.M. Bogdonoff‡
Princeton University, Princeton, New Jersey

Detailed hot-wire measurements of the longitudinal component of the mass-flow fluctuations have been made in an approximately self-preserving free shear layer reattaching on a 20-deg ramp at Mach number 2.9. The experimental configuration is especially designed to provide a well-defined initial condition for the reattachment process. The absolute mass-flow turbulence intensity increases dramatically through the compression in the reattachment region, which is in sharp contrast to similar subsonic reattachments. It is clear that the mean dilatation contributes significantly to the turbulence amplification. In addition, the length scale is affected strongly by the presence of extra strain rates. Prediction of this flow will require some sophisticated modeling, and the challenge to the predictor is clear.

Introduction

THE separation and reattachment of turbulent shear layers occurs in many practical situations. Typical examples include the flows on airfoils, and in diffusers, turbomachinery, etc. Although many studies have been performed, the physics of shear layer reattachment and the relaxation of the flow downstream of reattachment are still not well understood. One of the particular problems that hinder our understanding of the reattachment process is the possible coupling between separation and reattachment via the recirculating zone.

Recently, Settles et al. [1] described an experimental study of a reattaching turbulent free shear layer in a compressible flow. The test geometry was specifically designed such that the incoming free shear layer developed with a well-defined upstream history. The configuration was similar to a backward facing step, with one important difference (see Fig. 1). Instead of reattaching on a horizontal plane, the shear layer attached on a ramp, and the ramp was adjusted so that at the point where the upstream boundary layer separated, the flow direction did not change. As a result, no flow expansion or lip shock wave was present to affect the initial shear layer growth, and the reattachment occurred without these additional complications.

The mean flow data, and some preliminary hot-wire measurements of the mass-flow fluctuations, were presented by Settles et al.[1,2] Horstman et al.[3] compared these data with the results of a calculation method using a two-equation eddy viscosity turbulence model and concluded: "In general, the overall features of this complex flowfield have been predicted, although there are several areas of the flowfield in which significant improvements in the turbulence modeling are required if good agreement with experiment is to be achieved." Specifically, Horstman et al. found the length scale equation to be inadequate; in the shear layer, the turbulent length scale used was apparently too large, whereas downstream of reattachment, it seemed to be too small.

It is clear that further experimental work is required before we can claim to understand the turbulent, compressible reattachment process. The preliminary measurements of Settles et al., therefore, were repeated and extended, and the results of that work are presented here. The overall objective of this work is to gain more insight into the physics of the compressible shear layer reattachment and redevelopment process. With this understanding, it may be possible to construct new and/or improved turbulence models and, therefore, improve the performance of current calculation methods. To assist future work in this area, the raw data have been tabulated and they are available from the authors upon request.[4]

We begin by describing the apparatus and experimental techniques. The results, together with some preliminary discussion, are then presented, followed by the final discussion and conclusions.

Apparatus and Experimental Techniques

Wind Tunnel and Test Conditions

The experiment was conducted in the Princeton University 20×20-cm high Reynolds number supersonic wind tunnel at a freestream Mach number of 2.92 and a unit Reynolds number of 6.7×10^7/m. The wall conditions were near adiabatic.

The test model, shown in Fig. 1, was installed away from and parallel to the tunnel floor. A boundary layer developed initially on the upstream flat plate (229-mm long). Natural transition occurred within 30 mm of the plate leading edge and no tripping devices were used. At the point where the turbulent boundary layer separated over a backward facing step, the boundary-layer thickness δ_0 was about 3.5 mm with a Reynolds number based on momentum thickness of approximately 14,000. The free shear layer, formed by the separating boundary layer, bridged a 25.4-mm deep cavity before reattaching on a plane ramp. The ramp was inclined at 20 deg to the horizontal, and it was adjusted so that neither the pressure nor the flow direction changed when the boundary layer separated (see Fig. 2). For further details of the experimental configuration see Ref. 1.

The flowfield steadiness was investigated by Settles et al. using microsecond shadowgrams. In contrast to subsonic reattachment, where the reattachment line can move significantly, only a slight "tremble" of the wave system was observed. The magnitude of this wave motion was small compared to the average shear layer thickness and no large-scale unsteadiness seemed to be present.

Presented as Paper 83-0299 at the AIAA 21st Aerospace Sciences Meeting, Reno, Nev., Jan. 10-13, 1983; submitted Jan. 21, 1983; revision received Aug. 24, 1983.

*Research Associate, Mechanical and Aerospace Engineering Department, Gas Dynamics Laboratory. Member AIAA.

†Assistant Professor, Mechanical and Aerospace Engineering Department. Member AIAA.

‡Professor, Mechanical and Aerospace Engineering Department. Fellow AIAA.

Hot-Wire Measurement Technique

The hot-wire measurement technique was similar to that reported by Hayakawa et al.[5] A DISA 55M10 constant-temperature anemometer was used to measure the streamwise component of the mass-flow fluctuations. The probes were constructed by welding 5-μm tungsten wires to stainless steel support prongs. Some slack was given to the wire to avoid strain gaging, and the wire length was typically 1 mm.

The wires were calibrated for mass-flow sensitivity in a small Mach 3 pilot tunnel by changing the tunnel stagnation pressure. The temperature dependence of the mass-flow sensitivity was determined by repeating the calibration at several different resistance ratios. The calibration only applied where the mass-flow sensitivity was independent of Mach number, that is, where the local Mach number exceeded 1.2 (Ref. 6).

Under operating conditions, the system frequency response (deduced from a square-wave test) was typically 150 kHz or better. The operating overheat ratio varied between 1.0 and 1.3. Preliminary tests had shown that at these overheat ratios the contribution of the temperature fluctuations to the total signal was small, and it, subsequently, was neglected.

Digital analysis was used throughout. The mean and fluctuating components of the hot-wire signal were separated by appropriate filtering and digitized directly at sampling rates of 50 and 500 kHz, respectively. The raw data were stored on-line in the memory of a Hewlett-Packard HP1000 minicomputer for further processing. At each measurement point, data were taken as an ensemble of 25 records, each of which contained 1024 sampled points. Satisfactory convergence of fluctuation data was achieved with this record length (within 1% at $y/\delta = 0.5$). The instantaneous values of the anemometer voltage were converted directly to the instantaneous values of mass flow by inverting the calibration curve, thereby avoiding the use of sensitivity coefficients. The instantaneous mass-flow fluctuations were found by subtracting the time-averaged mass flow from the total instantaneous mass flow.

The difficulties of making accurate hot-wire measurements in compressible flows are well known. In this particular flow these difficulties were aggravated by the presence of thin shear layers and high-turbulence levels.

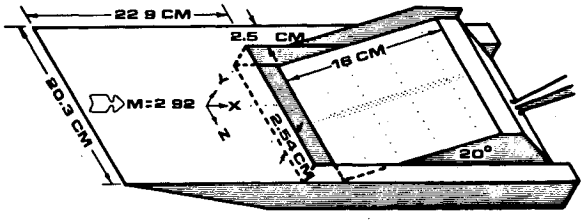

Fig. 1 Test model.

An error analysis indicates that the measurements were subject to both random and systematic errors. The random errors were associated with uncertainties in evaluating the sensitivity from the calibration curve and correcting the sensitivity for variations in stagnation temperature, in addition to the possibility of a drift in the hot-wire characteristics. Systematic errors included neglecting temperature fluctuations and mean stagnation temperature changes through the flowfield, as well as the errors due to the limited spatial and temporal resolution of the hot-wire system. These errors obviously varied through the flowfield, but an upper bound on the accuracy of $\overline{(\rho u)'^2}$ may be estimated by using the analysis of Smits et al.[7] For the present experiment, this analysis gives a possible error in $\overline{(\rho u)'^2}$ of -60% to -30% in the upstream boundary layer, and -22% to $+3\%$ downstream of reattachment. This estimate does not include errors due to the nonlinear behavior of the anemometer. Nonlinearities become important when the turbulence levels are high and, therefore, adversely affect the measurements near reattachment and further downstream. Nevertheless, we found that 1) the mean flow values were in good agreement with the pitot tube measurements reported earlier[2]; 2) the turbulence measurements were highly repeatable; and 3) the undisturbed shear-layer results fell within the scatter displayed by previous investigations. The upstream boundary-layer measurements, and most of the measurements in the free shear layer, are obviously only qualitatively useful. Yet, we feel that our measurements clearly capture the general characteristics of the turbulence behavior.

It should be mentioned that strain gaging was a particularly troublesome problem in the highly turbulent regions. The frequency spectrum of the hot-wire signal, therefore, was routinely checked and any suspect wires were discarded. By re-examining some of the earlier data presented in Refs. 1, 2, and 8, we found that some of those results were severely affected by strain gaging. All of the data presented in the current paper should, however, be free from these errors.

Measurement Positions

Hot-wire traverses were made at one station on the upstream flat plate, sixteen stations in the free shear layer, and nine stations downstream of reattachment. For convenience, the streamwise survey locations are identified by station numbers. Along the plate and free shear layer these stations start at a point 51 mm (2 in.) upstream of the separation lip, while stations on the ramp begin at its leading edge on the cavity floor. The station numbers are numerically equal to 0.395 times X mm (10.0 times X in.).

Results and Discussion

The results of the investigation reported in Refs. 1 and 2 may be briefly summarized as follows. The upstream turbulent boundary layer separates without deflection at the

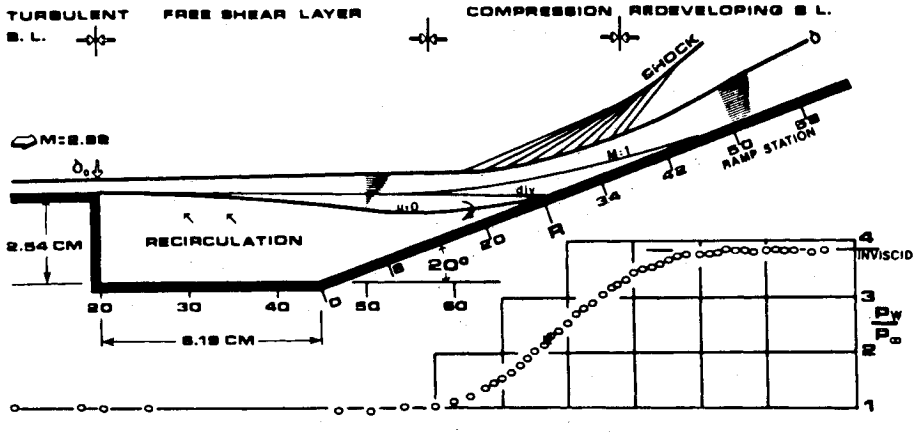

Fig. 2 Flowfield showing the surface static pressure distribution.

corner of the backward facing step, forming a free shear layer. The shear layer mean velocity profiles achieve self-similarity at station SH43, which is approximately $17\delta_0$ downstream of the step. The growth of the shear layer is faster on the low-speed side than on the high-speed side, and, as a result, reattachment occurs at a point slightly below the geometric extension of the flat plate on the ramp surface. The static pressure rises before reattachment and continues to rise well downstream. The compression waves associated with the shear layer curvature coalesce to form a shock wave in the freestream, at some distance outside the shear layers.

Downstream of the mean reattachment point (station R27) a new boundary layer begins to develop. The adverse pressure gradient in this region gradually reduces and becomes negligible at about station R44. The mean velocity near the wall rapidly increases with downstream distance and the wall-layer thickness grows quickly. The velocity profiles initially display a very large wake component (as may be expected) but this soon decreases. By station R42, the mean velocity appears to dip below the standard logarithmic law, suggesting that the length scale near the wall is abnormally large.[9,10] The relaxation of the boundary layer is certainly not monotonic. For instance, both the Clauser parameter G and the wake parameter π reach high values near reattachment but undershoot their respective equilibrium values of 6.8 and 0.55 downstream. This behavior agrees with that observed in many subsonic reattachment studies.[9,10]

The current investigation revealed that the turbulence behavior is in some ways even more spectacular. The profiles of the rms mass-flow fluctuation intensity $\langle(\rho u)'\rangle$ are shown in Figs. 3 and 4. Figure 5 shows the downstream evolution of the maximum intensity. In these figures the turbulence intensities are normalized by the mean freestream mass flow upstream of the reattachment to show the amplification of the absolute intensity. To interpret the results in terms of the local freestream mass-flow rate, it may be noted that the freestream mass-flow rate increases by 97% through the compression. The arrows in Figs. 3 and 4 indicate the sonic point locations. The results below these points should be ignored, since the hot-wire calibration is not valid in the transonic and subsonic regions.

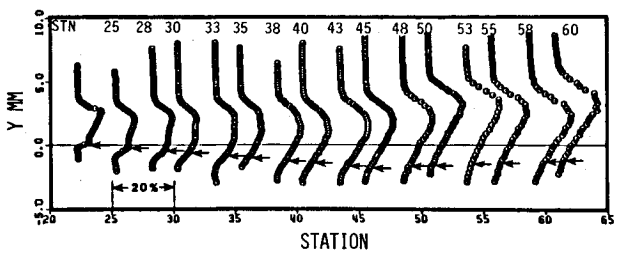

Fig. 3 Profiles of $\langle(\rho u)\rangle/(\overline{\rho U})_{ref}$ as a function of distance normal to the flow, free shear layer.

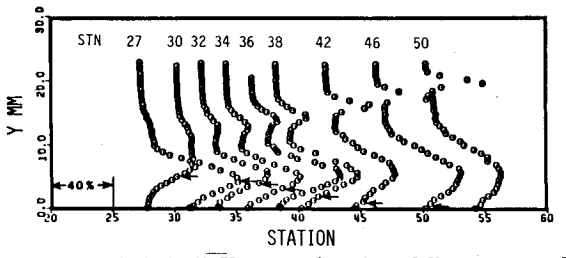

Fig. 4 Profiles of $\langle(\rho u)\rangle/(\overline{\rho U})_{ref}$ as a function of distance normal to the wall, downstream of reattachment.

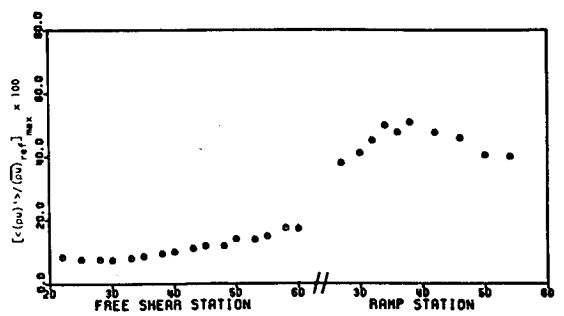

Fig. 5 Maximum value of rms mass-flow fluctuations vs distance along the flow.

As can be seen from these figures, the fluctuation intensity in the free shear layer increases slowly with downstream distance. In contrast to the mean flow measurements, it appears that the turbulence intensity profiles do not achieve similarity at any stage before reattachment. However, this observation may be incorrect. The relative temporal and spatial resolution of the hot wire improves with increasing shear-layer thickness, and this may give the erroneous impression that the turbulence intensity increases.

The maximum turbulence intensity rises rapidly as the shear layer approaches the ramp, and at reattachment it reaches a level of almost 40% (see Fig. 5). Downstream of this point, the intensity continues to rise before reaching a maximum at station R42 (which coincides closely with the point where the static pressure gradient becomes negligible).

This large increase in turbulence level, persisting downstream of reattachment, is rather unexpected. In subsonic flow, downstream of a backward facing step, it has been observed that the turbulence level reaches a peak before reattachment and then decays rapidly.[9-12] Chandrsuda and Bradshaw[10] suggested that this abrupt decrease in the Reynolds stresses is caused by the confinement of the large eddies by the normal component boundary condition $V=0$ at the solid surface. This "wall effect" increases the pressure strain term and the dissipation, while the triple products significantly decrease.

The observed increase in the dissipation rate is associated directly with a sharp decrease in the turbulence length scale. For instance, a typical length scale, such as the mixing length or the dissipation length scale, nearly halves near reattachment.[9] Apparently, as the large eddies from the free shear layer impinge on the wall, they either bifurcate[9] or they deflect alternately upstream and downstream. Even though the latter interpretation is supported by surface tuft measurements[11] and some low Reynolds number flow visualization work,[13] Bradshaw and Wong[9] have rejected it on the grounds that it would lead to strong unsteadiness. Yet the large eddies do display a considerable spread in frequency content, and strong unsteadiness need not result even if alternate deflection occurs near reattachment.

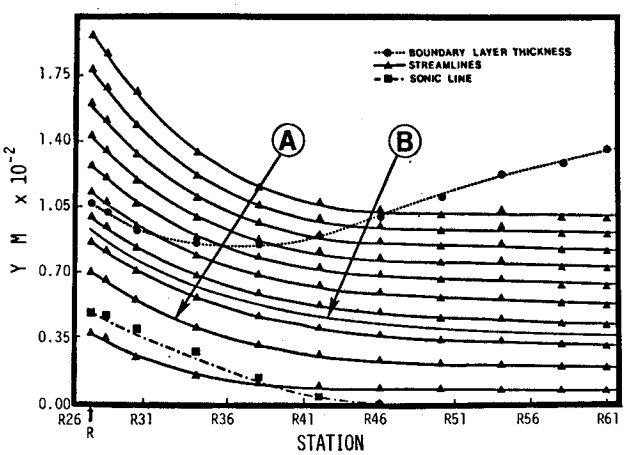

Fig. 6 Streamlines above the ramp.[24]

As we have already observed, compressibility radically alters the turbulence behavior near reattachment. In striking contrast to subsonic flows, the absolute turbulence intensity increases spectacularly through the reattachment region. To understand this behavior, we make qualitative use of the turbulent kinetic energy equation.

The turbulent kinetic energy equation describes the evolution of the normal stresses $\overline{u_i^2}(\equiv\overline{q^2})$ along a streamline; before it can be used to interpret the present measurements, however, a number of simplifications are required. In so doing, our approach broadly follows that of Bradshaw and Ferris[14] and Bradshaw.[15] First, we make the usual thin shear-layer approximations, even though these approximations probably break down in the interaction region. Second, in accord with Morkovin's hypothesis, we assume that $(\gamma-1)M^2$ is not much larger than unity, and that the divergence of the velocity fluctuations is zero (see Ref. 14 for further discussion). At this stage, we also ignore the effects of longitudinal curvature, high-turbulence intensity, and additional complications, such as shock oscillation. With these assumptions, the turbulent kinetic energy equation reduces to

$$\frac{D}{Dt}\left(\frac{1}{2}\overline{q^2}\right)=\underbrace{-\overline{u_iu_j}\frac{\partial U_i}{\partial x_j}}_{\text{(i)}}\underbrace{+\frac{\overline{\rho' u_j}}{\bar\rho^2}\frac{\partial\bar p}{\partial x_i}}_{\text{(ii)}}\underbrace{}_{\text{(iii)}}$$

$$\underbrace{-\epsilon}_{\text{(iv)}}\underbrace{-\frac{1}{\bar\rho}\frac{\partial}{\partial x_j}\left(\overline{p'u_j}+\frac{1}{2}\bar\rho\overline{q^2u_j}+\frac{1}{2}\overline{\rho' q^2u_j}\right)}_{\text{(v)}}$$

$$\underbrace{+\frac{\overline{q^2}}{\bar\rho}\frac{\partial}{\partial x_j}(\overline{\rho' u_j})}_{\text{(vi)}}\underbrace{+\frac{\overline{\rho' u_j}}{\bar\rho^2}\frac{\partial}{\partial x_j}(\bar\rho\overline{u_iu_j})}_{\text{(vii)}} \qquad (1)$$

Where both capital and lower case letters appear they represent mean and fluctuating velocities, respectively; overbars and primes are used to denote the mean and fluctuating parts of the pressure p and density ρ. The viscous diffusion has been neglected, and the symbol ϵ represents the dissipation rate.

Terms (v-vii) in Eq. (1) are generally small in a boundary layer except near its outer edge. Downstream of reattachment, however, these terms may not be small anywhere within the layer. Nevertheless, we focus our attention on the other four terms in Eq. (1).

The mean dilatation, $\partial U_i/\partial x_i(\equiv\mathrm{div}\,U)$ contributes to the production of turbulence through terms (ii) and (iii). Bradshaw[15] was able to write the mean dilatation contribution as a separate single term by making use of the following two considerations.

1) Morkovin's "strong Reynolds analogy," which implies that the instantaneous total temperature is constant and that the pressure fluctuations are negligibly small. This leads to

$$\rho'/\bar\rho\approx(\gamma-1)M^2(u/U) \qquad (2)$$

2) The continuity equation, for isentropic flow and thin shear layers. This gives

$$\mathrm{div}\,U\approx-\frac{U}{\gamma\bar p_w}\frac{d\bar p_w}{dx} \qquad (3)$$

where normal pressure gradients have been ignored and p_w is the static pressure measured at the wall.

By using $\overline{q^2}\approx2.5\overline{u^2}$, $\gamma=1.4$, and taking $\epsilon\equiv(-uv)^{3/2}/L$, where L is the dissipation length scale, Eq. (1) becomes

$$\frac{D}{Dt}\left(\frac{\overline{q^2}}{2}\right)=-\overline{uv}\frac{U}{y}-0.5\overline{q^2}\,\mathrm{div}\,U-(-\overline{uv})^{3/2}/L+\ldots \qquad (4)$$

As a final approximation we take $(-\overline{uv})/\overline{q^2}=a_1\approx0.15$. The evolution of $\overline{u^2}$ along a mean streamline is then given by

$$\frac{1}{\overline{u^2}}\frac{D\overline{u^2}}{Dt}=\alpha_1\frac{\partial U}{\partial y}-\alpha_2\mathrm{div}\,U-\alpha_3\frac{\overline{u^2}}{L}+\ldots \qquad (5)$$

where $\alpha_1=2a_1\approx0.3$, $\alpha_2=1.0$ and $\alpha_3=2a_1\sqrt{2.5a_1}\approx0.18$. The first term on the right-hand side is usually called the turbulence "production," the second represents the "total" contribution due to mean dilatation, and the third is the "destruction" of turbulence by dissipation.

Obviously, in arriving at Eq. (5), we have made a number of sweeping approximations, and the quantitative accuracy of this expression is therefore rather limited. Nevertheless, it represents a useful starting point for interpreting our present measurements. We begin by identifying two representative streamlines in the reattachment region, and proceed to estimate the relative magnitudes of the terms in Eq. (5).

Consider the two streamlines marked A and B in Fig. 6. The positions of these streamlines within the boundary layer, and the Mach number variations along them, are shown in Fig. 7. The evolution of the rms mass-flow intensity, as a fraction of the mass-flow rate upstream of the interaction, ρU_{ref}, is given in Fig. 8, and this figure also shows the implied variation of the velocity fluctuation intensity $\langle u'\rangle/\bar U_{\mathrm{ref}}$ [calculated by using the strong Reynolds analogy, Eq. (2)].

The initial rise in turbulence levels along the two streamlines is quite different, but the behavior downstream of station R38 is very similar. The reasons may be found by

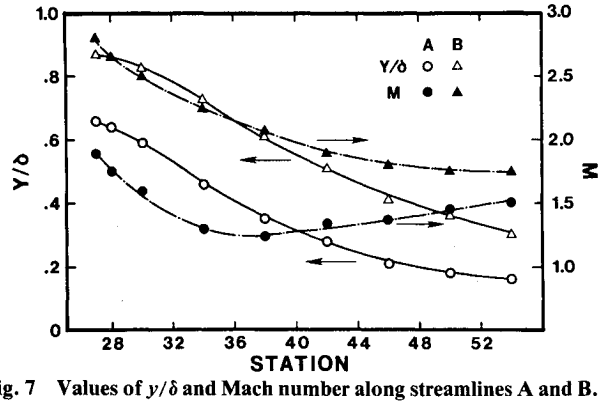

Fig. 7 Values of y/δ and Mach number along streamlines A and B.

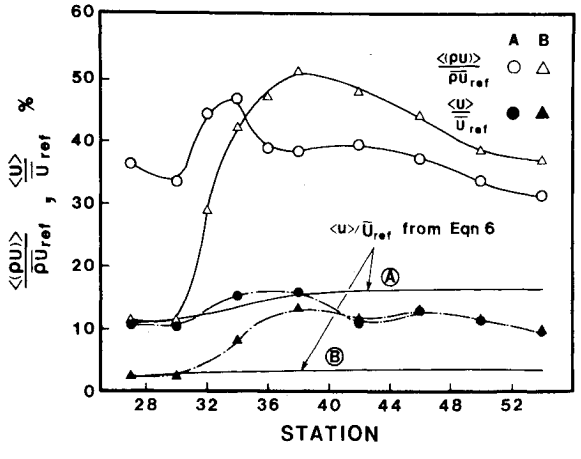

Fig. 8 Longitudinal mass-flow and velocity fluctuation intensity along streamlines A and B.

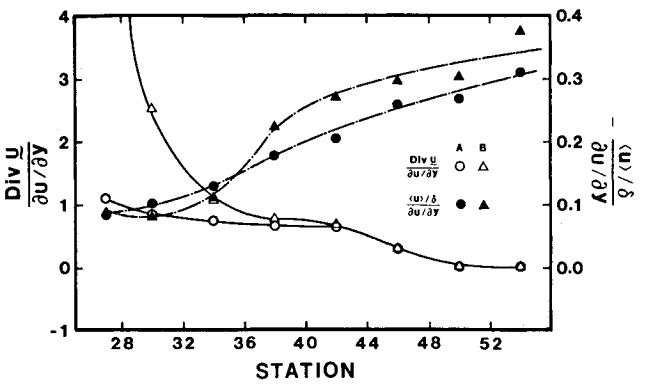

Fig. 9 $\mathrm{div}U/(\partial U/\partial y)$ and $-(\langle u\rangle/\delta)/(\partial U/\partial y)$ along streamlines A and B.

evaluating the relative magnitudes of the terms in Eq. (5). For instance, the variation of $\mathrm{div}U/(\partial U/\partial y)$ along the two streamlines [calculated using Eq. (3) and the experimental results] is shown in Fig. 9. The dilatation term evidently overwhelms the production term for a considerable distance downstream, particularly along streamline B.§ To find the relative magnitude of the dissipation term, it is necessary to know the dissipation length-scale distribution. This information is unfortunately not available. Some indication of the dissipation behavior, however, is given by the variation of $(\sqrt{u^2}/\delta)/(\partial U/\partial y)$. Figure 9 shows that along both streamlines this ratio rises rapidly downstream of reattachment, which perhaps suggests that the dissipation rate also increases.

Consider the case where the dilatation term dominates the right-hand side of Eq. (5). In this case we obtain a simple algebraic expression for the variation of $\overline{u^2}$ along a mean streamline (see, for example, Ref. 16). That is

$$\overline{u^2}/\bar{\rho} = \text{const} \tag{6}$$

A relationship similar to Eq. (6) was derived by Dussauge and Gaviglio.[16] They found that it accurately described the behavior of $\overline{u^2}$ in a rapid, 12 deg expansion of a turbulent boundary from an initial Mach number of 1.76. [They considered the two contributions to the dilatation term separately; Eq. (6) closely approximates their final result.] Nevertheless, when Eq. (6) was applied along streamlines A and B in the current experiment, the increase in $\overline{u^2}$ was overestimated along A and underestimated along B (see Fig. 8).

When we look at the full equation this result is not really surprising. For example, streamline B is initially located close to the shear-layer edge and the other terms in Eq. (1) are obviously important [particularly the extra "generation" terms (vi) and (vii) which have been ignored thus far]. In addition, along streamline A, the dissipation and, possibly, the "diffusion" [term (v) in Eq. (1)] are important.

In summary, all the terms in Eq. (1) may be important at a given point in the flow, and the observed turbulence behavior is the result of many competing influences. What cannot be denied, however, is the strong amplification effect of the mean dilatation, and a successful prediction method will require careful treatment of the terms containing $\mathrm{div}U$.

In addition to contributing explicitly to the turbulent kinetic energy balance, the mean dilatation appears to have a strong effect on the turbulence length scale. Bradshaw[15,17] suggested that the mean dilatation can be considered as an "extra" strain rate similar to longitudinal streamline curvature and streamline divergence. In the context of a turbulence model

§Dilatation/production $= -\dfrac{\alpha_2}{\alpha_1}\dfrac{\mathrm{div}U}{\partial U/\partial y}$ and $\dfrac{\alpha_2}{\alpha_1}\approx 3$.

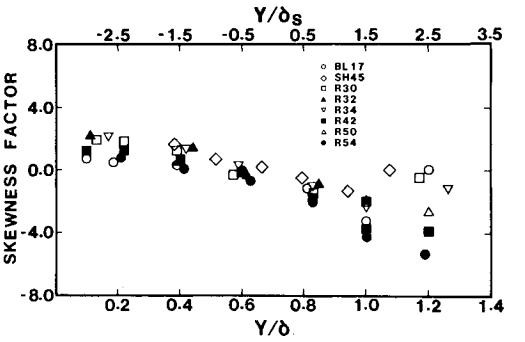

Fig. 10 Skewness factor distributions.

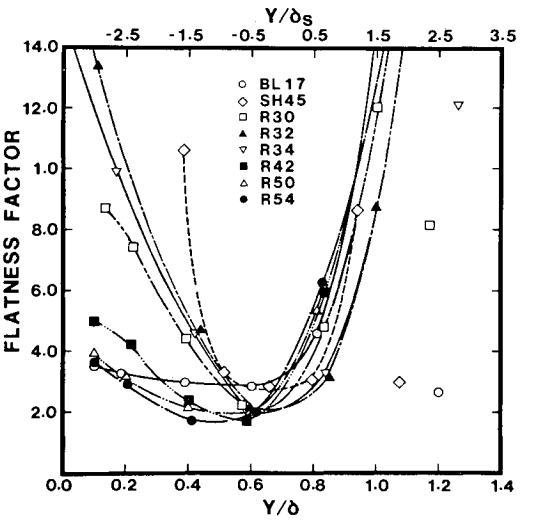

Fig. 11 Flatness factor distributions.

based on the turbulent kinetic energy equation, these extra strain rates significantly affect structure parameters such as the dissipation length scale. In fact, for a small, constant extra strain rate e, the length scale appears to change by a factor F, where

$$F = 1 + \alpha_0 \frac{e}{\partial U/\partial y} \tag{7}$$

The value of α_0 depends to some extent on the nature of the extra strain rate, but it is generally of 0(10). For dilatation $e = -\mathrm{div}U$, and for concave curvature $e = -\partial V/\partial x$.

In the present experiment, the extra strain rates vary with streamwise distance (see, for instance, Fig. 9), and they are only significant over times comparable to a typical eddy lifetime (that is, a distance approximately equal to 10). For such impulsively applied extra strain rates, Smits et al.[18] proposed that the effective, total amplification factor was given by

$$F = 1 + \alpha_0\theta \tag{8}$$

where $\theta \equiv \int e\,dt$, and θ was assumed to be small. For an impulse in concave curvature, θ is positive and approximately equal to the total turning angle.[18] For an impulse in dilatation, Eq. (3) gives $\theta = (1/\gamma)\ln(p_2/p_1)$, where p_2/p_1 is the static pressure rise through the interaction.[8]

When we consider only the dilatation effect caused by the compression at reattachment, we find that $\theta \approx 0.9$. The predicted increase in dissipation length scale, therefore, is very large indeed; a factor of seven at least (using $\alpha_0 = 7$, which seems the best estimate for the dilatation extra strain rate when the true dilatation terms are modeled separately).

Of course, these large values of θ violate the conditions under which a simple F-factor approach applies. Yet, Smits et al.[18] found, for an impulse in concave curvature with θ as large as 0.3, this simple analysis gave a plausible description of the observed results. In addition, Horstman et al.[3] found that, in the present case, an arbitrary increase in the length scale, equivalent to increasing the ordinary flat plate value by a factor of six, considerably improved agreement between the calculated and the experimental velocity profiles. Thus, the simple F-factor approach may still have application for relatively large impulsive extra strain rates.

In the preceding discussion, the effect of streamline curvature has been ignored. Nevertheless, this effect is not necessarily small, since the total turning angle is 20 deg, and the corresponding value of θ is approximately 0.3. Like dilatation, concave curvature acts to increase the length scale, and the preceding simple analysis suggests that the two effects add linearly. Considerable evidence exists to the contrary[19,20]; the effect of more than one extra strain rate rarely seems to be cumulative. In fact, if dilatation acts like streamline divergence (as has been tentatively suggested in Ref. 17), the results of Smits et al.[19] imply that the presence of concave curvature inhibits the effect of dilatation. The actual increase in the dissipation length scale, therefore, is expected to be smaller than if only dilatation was present.

The turbulence length scale will also be strongly affected by the possibility of either large eddy bifurcation near reattachment, or the equivalent mechanism of alternate deflection upstream and downstream. As we have already mentioned, either mechanism provides an explanation for the sharp decrease in length scale that is observed in incompressible reattaching flows. It seems likely that a similar effect occurs in a compressible reattaching flow, but it will be obscured by the presence of large extra strain rates. The combined effect of bifurcation and destabilizing extra strain rates probably means that the total increase in dissipation length scale is less than that predicted on the basis of the extra strain rates acting alone. In fact, if we use a local equilibrium argument at station R54, we find that for both streamlines the inferred dissipation length scale is approximately twice the equilibrium boundary-layer value. Of course, this estimate for L is rather inaccurate because the boundary layer is far from equilibrium. Nevertheless, the evidence suggests that the overall change in length scale is the combined effect of bifurcation (or similar mechanism) and competing extra strain rates. The end result seems to be a considerable increase in length scale through the interaction.

It has been suggested that a structure parameter such as the length scale takes some time to respond to the application of an extra strain rate.[17,18] Similarly, it will take some time to respond to the removal of the extra strain rate. According to the simple lag formulation that led to Eq. (8), the length scale relaxes exponentially to its equilibrium value, with a typical relaxation length of approximately 10δ. This implies a slow relaxation; in the present experiment the relaxation is only just beginning at station 50 and little or no information about this process, therefore, is available.

Further interesting characteristics of the flow are visible in the higher order moments. Consider the skewness and flatness factor distributions shown in Figs. 10 and 11. To allow a comparison between the results for the boundary layer and the shear layer, the horizontal scales in Figs. 10 and 11 were conveniently adjusted. Note that points in the transonic regime have been retained because the nondimensional higher

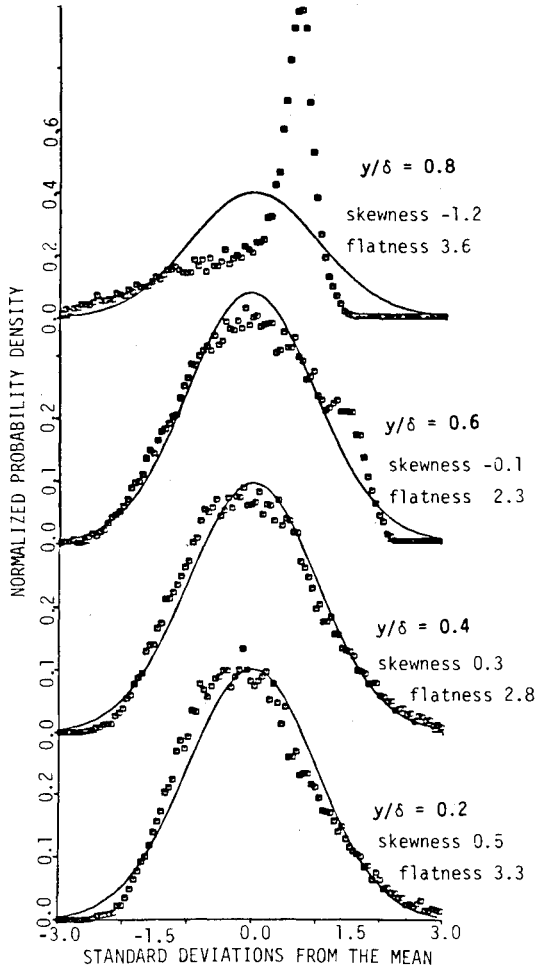

Fig. 12 Probability density distributions, typical Mach 2.9 flat plate boundary layer.[5]

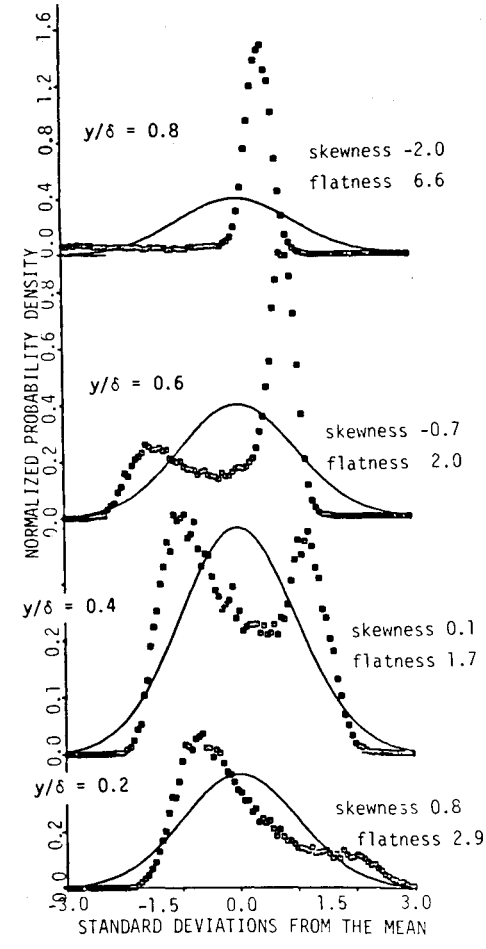

Fig. 13 Probability density distributions downstream of reattachment, station R54.

order moments are relatively weak functions of the wire calibration.

The flat plate distributions (BL17) exhibit the usual characteristics of an equilibrium boundary layer, which, apparently, is independent of Mach number for nonhypersonic flows (see, for instance, Ref. 5). Similarly, the free shear-layer results bear a strong resemblance to the incompressible mixing layer data of Wygnanski and Fiedler.[21] The boundary layer just downstream of reattachment clearly retains this mixing layer character, but as we proceed downstream, the influence of the wall becomes more apparent. In particular, the flatness factor near the wall decreases rapidly and at the last measurement station (R54) it approaches the flat plate boundary-layer values.

It was not possible to detect a change in the integral time scale through the interaction because this was obscured by scatter in the spectral data at low frequencies. Shadowgraphs, however, appear to indicate that the length scale of the turbulent motions increases, thus supporting our interpretation of the turbulence behavior downstream of reattachment.

Further evidence for the presence of abnormally large length scales is provided by the probability density distributions. The results for the flat plate boundary layer prior to separation are shown in Fig. 12, and for the boundary layer downstream of reattachment in Fig. 13. Clearly, the freestream fluid penetrates much deeper into the layer after reattachment, indicating the presence of large-scale motions. By bringing fluid with a relatively high mass-flow rate close to the wall, these deep intrusions are responsible for the rapid decrease of the velocity profile wake component.

The increased length scale downstream of reattachment can also be inferred from the fourth-order moment results. The location where the minimum in flatness factor occurs tends toward the wall after reattachment (see Figs. 11-13), which suggests the increased intermittent region, which in turn indicates the presence of large-scale motions.

Conclusions and Final Discussion

We have presented measurements of the mass-flow fluctuations in a compressible reattaching flow where the incoming shear layer was approximately self-preserving before reattachment. The most distinguishing feature observed was a dramatic increase in turbulence intensity near reattachment, which was in sharp contrast to that observed in similar incompressible flows. By using an approximate form of the turbulent kinetic energy equation, we demonstrated that mean dilatation significantly contributed to the amplification of the turbulence intensities. The overall flow behavior, however, was far from simple, and many competing influences were present. In particular, the turbulence length scale appeared to be both reduced by eddy bifurcation near reattachment and amplified by the action of extra strain rates due to dilatation and longitudinal curvature. In our analysis we ignored the possibility of turbulence amplification caused by unsteady oscillation of the wave system, and by local deformation of the compression waves by the turbulence itself. Several authors[22,23] have suggested that these mechanisms may be important. In short, successful prediction of the present flow will require some very sophisticated modeling, and the challenge to the predictor is clear.

Acknowledgments

This work was supported by NASA Headquarters, Grant NAGW-240, monitored by Drs. Clint Brown and Gary Hicks.

References

[1] Settles, G.S., Baca, B.K., Williams, D.R., and Bogdonoff, S.M., "Reattachment of a Compressible Turbulent Free Shear Layer," *AIAA Journal,* Vol. 20, Jan. 1982, pp. 60-67.

[2] Settles, G.S., Baca, B.K., Williams, D.R., and Bogdonoff, S.M., "A Study of Reattachment of a Free Shear Layer in Compressible Turbulent Flow," AIAA Paper 80-1408, 1980.

[3] Horstman, C.C., Settles, G.S., Williams, D. R., and Bogdonoff, S.M., "A Reattaching Free Shear Layer in Compressible Turbulent Flow—A Comparison of Numerical and Experimental Results," AIAA Paper 81-0333, 1981.

[4] Hayakawa, K. and Smits, A.J., "Compilation of Turbulence Data for a Reattaching Shear Layer at Mach 2.9," Princeton University, Princeton, N.J., MAE Rept. 1601, April 1983.

[5] Hayakawa, K., Smits, A.J., and Bogdonoff, S., M., "Hot-Wire Investigation of an Unseparated Shock-Wave/Turbulent Boundary Layer Interaction, " AIAA Paper 82-0985, 1982. Also, *AIAA Journal,* 1984, in press.

[6] Kovasznay, L.S.G., "The Hot-Wire Anemometer in Supersonic Flow," *Journal of Aeronautical Sciences,* Vol. 17, 1950, pp. 565-573.

[7] Smits, A.J., Hayakawa, K., and Muck, K.C., "Constant-Temperature Hot-Wire Anemometer Practice in Supersonic Flows, Part I—The Normal Wire," *Experiments in Fluids,* Vol. I, 1983, pp. 83-92.

[8] Hayakawa, K., Smits, A.J., and Bogdonoff, S.M., "Turbulent Measurements in Two Shock-Wave/Shear Layer Interactions," *IUTAM Symposium on Structure of Complex Turbulent Shear Flow,* Marseilles, edited by R. Dumas and L. Fulachier,Aug.-Sept. 1982, Springer Verlag, Berlin, 1983, pp. 279-288..

[9] Bradshaw, P. and Wong, F.Y.F., "The Reattachment and Relaxation of a Turbulent Shear Layer," *Journal of Fluid Mechanics,* Vol. 52, 1972, pp. 113-135.

[10] Chandrsuda, C. and Bradshaw, P., "Turbulence Structure of a Reattaching Mixing Layer," *Journal of Fluid Mechanics,* Vol. 110, 1981, pp. 171-194.

[11] Kim, J., Kline, S.J., and Johnston, J.P., "Investigation of Separation and Reattachment of a Turbulent Shear Layer: Flow over a Backward-Facing Step," Thermosciences Div., Dept. of Mechanical Engineering, Stanford University, Stanford, Calif., Rept. MD-37, 1978.

[12] Eaton, J.K. and Johnston, J.P., "An Evaluation of Data for the Backward-Facing Step Flow," Report prepared for the 1980/81 Stanford Conferences on Complex Turbulent Flows, Stanford University, Stanford, Calif., 1980.

[13] Smits, A. J., "A Visual Study of a Separation Bubble," *Flow Visualization II,* Hemisphere Publishers, N.Y., 1982, pp. 247-251.

[14] Bradshaw, P. and Ferriss, D.H., "Calculation of Boundary-Layer Development Using the Turbulent Energy Equation: Compressible Flow on Adiabatic Walls," *Journal of Fluid Mechanics,* Vol. 46, 1971, pp. 83-110.

[15] Bradshaw, P., "The Effect of Mean Compression or Dilatation on the Turbulence Structure of Supersonic Boundary Layers," *Journal of Fluid Mechanics,* Vol. 63, 1974, pp. 449-464.

[16] Dussauge, J.P. and Gaviglio, J., "Bulk Dilatation Effects on Reynolds Stresses in the Rapid Expansion of a Turbulent Boundary Layer at Supersonic Speeds," *Proceedings of the Third Symposium on Turbulent Shear Flows,* University of California, Davis, Calif., Sept. 1981, pp. 2.33-2.38.

[17] Bradshaw, P., "Effects of Streamline Curvature on Turbulent Flow," AGARDograph 169, 1973.

[18] Smits, A.J., Young, S.T.B., and Bradshaw, P., "The Effect of Short Regions of High Surface Curvature on Turbulent Boundary Layers," *Journal of Fluid Mechanics,* Vol. 94, 1979, pp. 209-242.

[19] Smits, A.J., Eaton, J.A., and Bradshaw, P., "The Response of a Turbulent Boundary Layer to Lateral Divergence," *Journal of Fluid Mechanics,* Vol. 94, 1979, pp. 243-268.

[20] Smits, A.J. and Joubert, P.N., "Turbulent Boundary Layers on Bodies of Revolution," *Journal of Ship Research,* Vol. 26, 1982, pp. 135-147.

[21] Wygnanski, I. and Fiedler, H.E., "The Two-Dimensional Mixing Region," *Journal of Fluid Mechanics,* Vol. 41, 1970, pp. 327-361.

[22] Anyiwo, J.C. and Bushnell, D.M., "Turbulence Amplification in Shock-Wave Boundary-Layer Interaction," *AIAA Journal,* Vol. 20, 1982, pp. 893-899.

[23] Zang, T.A., Hussaini, M.Y., and Bushnell, D.M., "Numerical Computations of Turbulence Amplification in Shock Wave Interactions," AIAA Paper 82-0293, 1982.

[24] Baca, B.K., M. Sc. Dissertation, Princeton University, Princeton, N.J., 1981.